Poster paper

Enhanced CASSI Snapshot Imager Using Dual Prism Dispersion

Ding M, Yuen PWT*, Piper J, Soori U, Selvagumar S, Gunes M and Zahidi U

*Email: p.yuen@cranfield.ac.uk

Centre for Electronic Warfare, Information & Cyber (EWIC), Cranfield University, Defence Academy of UK, Shrivenham SN6 8LA

Abstract: Conventional Coded Aperture Snapshot Spectral Imager (CASSI) utilises coded aperture as a spatial modulator and it normally employs a single prism or a compound Amici prism for spectral dispersion to realise the acquisition of spectral and spatial data in a single shot simultaneously. The optics of the CASSI system is designed such that a pre-defined spectral range of the dispersed voxel of each element is sensed by a desire number of sensor pixels. While CASSI system has been shown to be effective for snap shot multispectral imaging application, one main drawback in the CASSI system is the wavelength dependent spectral resolution due to the non-linear dispersions in the employed dispersive optics. The single prism design suffers from anamorphic distortion and the double Amici prism exhibits rather strong wavelength dependent dispersion which limits only a certain fixed set of spectral wavelengths to be usable in the system.
In this paper, we proposed a new design of an agile dispersive element using a pair of prisms which enables tuneable spectral wavelengths for the snap shot multispectral imaging system without the need of hardware modification. The less number of dispersion element utilised in this design also helps to reduce transmission loss. The work reported here has been carried out by ray tracing (TracePro) and the performance of the system is assessed by Matlab.

I. INTRODUCTION

Snapshot multi-spectral imaging has been a highly-efficient technique for remote sensing application in great contrast to the conventional push broom scanning system [1]–[3]. Spectral sensing has wide range of applications e.g. computed tomography imaging in medical examination[4], imaging spectrometer in ophthalmology[5], image slicing spectrometer in microscopy[6] and many other industrial applications[7]–[10].

Among those, coded aperture snapshot spectral imaging system exploits the theory of compressive sensing with a simple combination of the coded aperture mask as spatial modulator and a spectrograph as spectral modulator to acquire the spatial data and spectral data simultaneously[11]. Extensive studies on snap-shot imaging such as the Coded Aperture Snapshot Spectral Imager (CASSI) have been widely reported [12]–[17]. Almost all CASSI system studied so far utilised prism based dispersion element, such as the single prism [12] and the double Amici prism [18,21]. The CASSI design not only suffering from strong chromatic aberrations and astigmatisms, the non-linear dispersion of the prism makes the system only useable for a set of fixed wavelengths. For instance, in the Amici based CASSI it selects only the wavelengths of light that are dispersed in the tangential plane onto the unit pixels of the focal plane array for image recovering. The system is constraint to be useable only for this set of wavelengths which is set according to the dispersion characteristics of the dispersive Amici [18]–[20]. It is well-known that optimum target detection performance is critically dependent on the utilisation of 'appropriate' wavelengths of the spectral imagery, and furthermore different scenes with different backgrounds will need different sets of wavelengths for optimal target detection. The fixed wavelength in the current CASSI design limits its usefulness for practical application. This paper proposes to implement a pair of prisms as the spectrograph of the CASSI that will enable tuneable wavelength without hardware modification. Remaining issues such as chromatic aberrations will be addressed in the future work.

II. SYSTEM MODEL

CASSI system with a single disperser, also called SD CASSI, consists of several relay optics, one coded aperture mask and one dispersive element as shown in Fig.1.

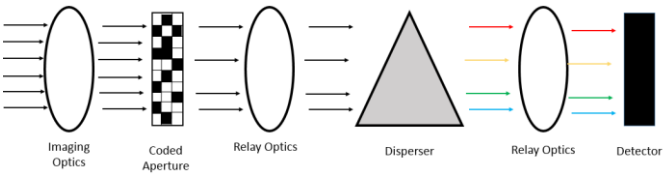

Fig. 1 Schematic of SD CASSI

At the entrance, an imaging lens is to form the image to the system from the scene. The incident rays are filtered by the coded aperture mask in spatial domain. The rest of rays go through the dispersive element and at the end project onto the detector plane. The relay optics in between are the bridges to transfer the image.

Assume that the spectral density at the entrance can be represented as $S_0(x, y, \lambda)$ where x and y are spatial coordinates and λ denotes the wavelength. The spectral density after coded aperture is

$$S_1(x, y, \lambda) = S_0(x, y, \lambda) * C(x, y) \quad (1)$$

where $C(x, y)$ denotes the coded aperture mask in 2 dimensions. After the dispersive element, the spectral density is

$$S_2(x, y, \lambda) = S_0(x, y + \alpha(\lambda - \lambda_c), \lambda)$$

$$* C(x, y + \alpha(\lambda - \lambda_c)) \quad (2)$$

where the additional part $\alpha(\lambda - \lambda_c)$ represents the spatial shift dependent on the difference between the current wavelength and central wavelength. In equation (2), it assumes the shift happens along y axis. α denotes the dispersive coefficient. Theoretically, if α is a constant, the dispersion will be linear and thus all the channels can be recovered with the minimum spectral resolution. However, in the experiment, this coefficient commonly is not a constant any more. Non-linear dispersion often exists in the prism-based system.

In the first SD CASSI prototype using single equilateral prism[12] as shown in Fig. 2, a bundle of rays in multiple wavelengths propagating in a single prism are dispersed according to the Snell's law.

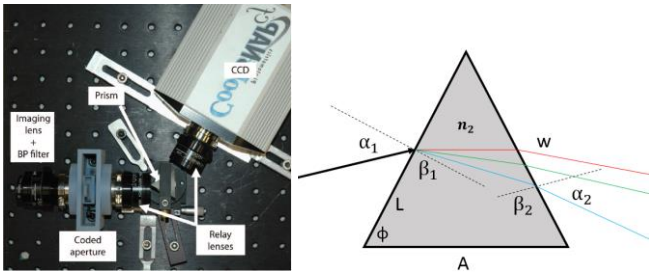

Fig. 2 First SD CASSI prototype[12] (left); Light prorogation in single equilateral prism (right)

Snell's law demonstrates how the refraction happens, which is

$$n_1 \sin(\alpha) = n_2 \sin(\beta) \quad (3)$$

where α denotes incident angle and β denotes the refractive angle. n_1 and n_2 denote the refractive index of two intermedia respectively. From Fig. 2 (right), the exit rays exhibit dramatic refraction angular difference with respected to the incident one, which deviates the optical axis of the exit ray from that of the incidence inducing strong spherical and chromatic aberration in the single-prism system. This makes the single prism as the sole dispersion element in the CASSI not practical for a real system.

In the second CASSI prototype [18][21] a double amici is introduced to keep the central wavelength undeviated through the prism as shown in Fig. 3.

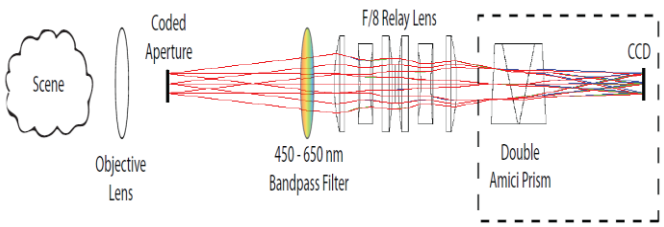

(a)

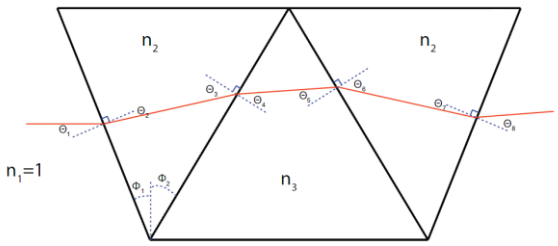

(b)

Fig. 3 (a) Schematic of 2nd prototype of SD CASSI[18]; (b) Diagram for undeviated central wavelength in double amici prism[21]

The Amici is designed to solve the off-axis problem in the single prism system such that the dispersion will be symmetrically distributed in the tangential plane with respected to a central wavelength. However, the non-linear dispersion in the Amici also limits a fixed set of wavelength to be usable in the imaging system.

Fig. 4 shows the ray diagram of the proposed design by using two identical prisms which are placed in parallel to allow flexible wavelength for imaging by adjusting the air gaps between the two prisms. The relationships of the incident angles, refractive angles and exit angles in this Dual-prism system are described as follows,

$$\sin(\alpha_1) = n_2 * \sin(\beta_1) \quad (4)$$

$$\beta_2 = 180° - \varphi_1 - \varphi_2 - \beta_1 \quad (5)$$

$$\sin(\alpha_2) = n_2 * \sin(\beta_2) \quad (6)$$

$$\alpha_3 = \alpha_2 \quad (7)$$

$$\sin(\beta_3) = \sin(\alpha_3)/n_2 \quad (8)$$

$$\beta_4 = 180° - \varphi_1 - \varphi_2 - \beta_3 \quad (9)$$

$$\sin(\alpha_4) = n_2 * \sin(\beta_4) \quad (10)$$

From equations (4) – (10) we can find α_1 and α_4 are equal where there is no angular difference between incident angle and exit angle and only the optical axis is shifted along the tangential plane. The improvement of CASSI system takes the advantage of this feature. Besides, the two prisms help to improve light transmission in comparison to that of the Amici system.

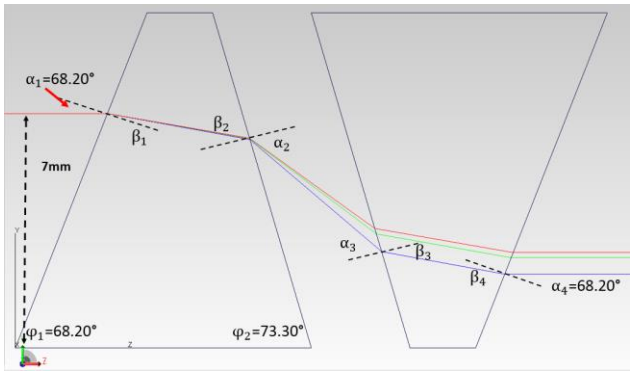

Fig. 4 Ray tracing of Dual-prism system in TracePro; incident angle $\alpha_1 = 68.20°$, incident height H = $7mm$, bottom angles of the prism $\varphi_1 = 68.20°$ and $\varphi_2 = 73.30°$ and exit angle $\alpha_4 = 68.20°$

III. SIMULATIONS AND ANALYSIS

Since the focus of an optical imaging system can be better located by using beams with a range of incident angles, this experiment utilises 4° incident angle range and the ray tracing result is shown in Fig. 6. It is seen that three different incident beams of 550nm wavelength intersect not in a single focus point. This error can be minimized within the tolerance of a pixel by varying the design parameters.

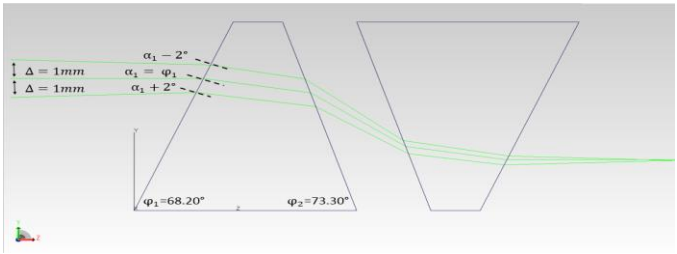

Fig. 6 Ray tracing of Dual-prism system in TracePro; 3 rays at 550nm enter the prism with the incident angle 66.20°, 68.20° and 70.20°, respectively. The height difference between the sources Δ is 1mm width

Meanwhile, multiple wavelengths in the system generate the axial shift so that the focal plane could not be a plane any more. Fig. 7 demonstrates the axial shift of three beams in three wavelengths (400nm, 550nm, and 700nm).

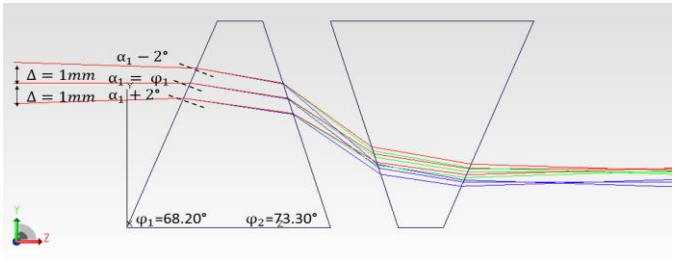

Fig. 7 Ray tracing of Dual-prism system in TracePro; three incident rays in a bundle at 400nm, 550nm and 700nm with the incident angle 66.20°, 68.20° and 70.20°, respectively. The height difference between the sources is 1mm width

Since the equations (4) - (10) are extended to two prisms and multiple wavelengths, the axial shift and multiple focal points can be balanced in Matlab to find out the best system parameters. According to the calculations, the dual-prism system is design as $\varphi_1 = 85.9°$, $\varphi_2 = 73.7°$, A = 7.5mm, height = 20mm and initial air gap = 5.8484mm (the prism angles are referred from [21]). Fig. 8 shows the overview of Dual-prism system and its ray tracing result.

Table 1 Comparison of displacement of Dual-prism System (N-BK7) with three different gaps and UV-CASSI reference data

Band	Dual-prism System Air gap + 0mm	Dual-prism System Air gap + 5mm	Dual-prism System Air gap + 10mm	UV-CASSI System
400nm	-0.0357mm	-0.0638mm	-0.0919mm	-0.2117mm
450nm	-0.0197mm	-0.0351mm	-0.0506mm	-0.1208mm
500nm	-0.0083mm	-0.0149mm	-0.0215mm	-0.0526
550nm	0mm	0mm	0mm	0mm
600nm	0.0065mm	0.0115mm	0.0166mm	0.0426mm
650nm	0.0116mm	0.0207mm	0.0298mm	0.0753mm
700nm	0.0158mm	0.0282mm	0.0406mm	0.1051mm

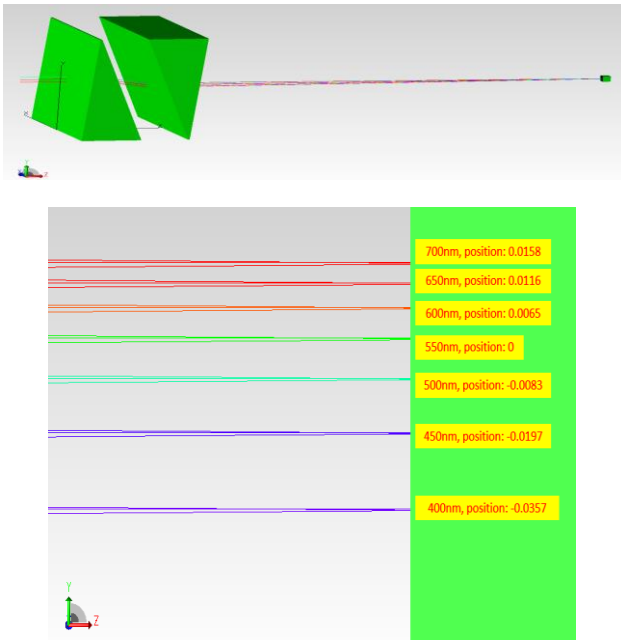

Fig. 8 Ray tracing of Dual-prism (N-BK7) system in TracePro; $\varphi_1 = 85.90°$ and $\varphi_2 = 73.70°$, the length of prism bottom is 7.5mm, prism height is 20mm, initial air gap is 5.8484mm, the incident angle range 0.8°, central light source height is 10mm and the height difference between sources $\Delta = 0.5$mm

By varying the distances between two prisms it is shown in Fig. 9 that the relative dispersion width @ 400nm – 700nm is seen to vary when the air gap is adjusted from +0mm to +10mm with 1mm increment in this Dual-prism system (N-BK7) compared with Ultraviolet-Visible CASSI (UV-CASSI) data. The central point is set at 550nm for the range of 400-700nm. Table 1 shows the dispersion with air gap parameters. Concretely, seven wavelengths spread in a range of 51.5μm, 92μm and 132.5μm under +0mm air gap, +5mm air gap and +10mm air gap respectively. With the length of the air gap changed, the relative position of each wavelength to the central wavelength is not same any more. It reflects the change of acquired spectral channels on the detector. At this point, multi-shot with the varied air gap helps the system to make up the missing spectral channels for the further reconstruction. Hence, the structure of two prisms potentially upgrades CASSI system to be more dynamic than the conventional CASSI design. Although, UV-CASSI system has a larger range of the dispersion on the spatial domain in Table 1, note that the CASSI system has already been optimized by the lens design system and the optimization of Dual-prism system will be carried on in the future work to make the system become more functional.

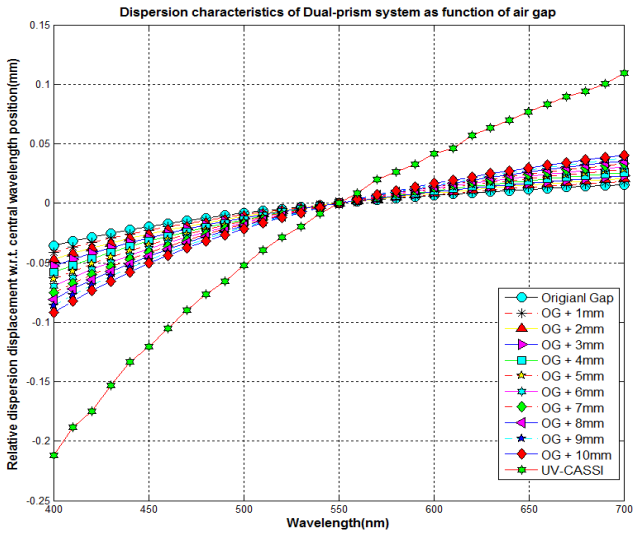

Fig. 9 Dispersion result @ 400nm – 700nm varied with Air gap (+0 – 10mm) and UV-CASSI result

IV. CONCLUSION

This paper proposed a new design by using a dual-prism structure for the improvement of SD CASSI system. Dual-prism system reduces anamorphic and chromatic distortions in comparison to that of the single prism and Amici in the CASSI system. The optical axis of the dual-prism in the sagittal plane is retained when they are placed in parallel. The main contribution of this work as shown in Fig. 9 is the demonstration of flexible wavelengths that can be useable in the CASSI system through the adjustment of the air gap between the two prisms. The issue of aberration reduction in the dual-prism CASSI will be addressed in the future work.

V. REFERENCE

[1] N. Hagen and M. W. Kudenov, "Review of snapshot spectral imaging technologies," *Opt. Eng.*, vol. 52, no. 9, p. 90901, 2013.

[2] N. Hagen, "Snapshot advantage: a review of the light collection improvement for parallel high-dimensional measurement systems," *Opt. Eng.*, vol. 51, no. 11, p. 111702, 2012.

[3] L. Gao and L. V. Wang, "A review of snapshot multidimensional optical imaging: Measuring photon tags in parallel," *Phys. Rep.*, vol. 616, pp. 1–37, 2016.

[4] J. R. Weber, D. J. Cuccia, W. R. Johnson, G. H. Bearman, A. J. Durkin, M. Hsu, A. Lin, D. K. Binder, D. Wilson, and B. J. Tromberg, "Multispectral imaging of tissue absorption and scattering using spatial frequency domain imaging and a computed-tomography imaging spectrometer.," *J. Biomed. Opt.*, vol. 16, no. 1, p. 11015, 2008.

[5] W. R. Johnson, D. W. Wilson, W. Fink, M. Humayun, and G. Bearman, "Snapshot hyperspectral imaging in ophthalmology.," *J. Biomed. Opt.*, vol. 12, no. 1, p. 14036, 2014.

[6] L. Gao, R. T. Kester, and T. S. Tkaczyk, "Compact Image Slicing Spectrometer (ISS) for hyperspectral fluorescence microscopy.," *Opt. Express*, vol. 17, no. 15, pp. 12293–12308, 2009.

[7] Cuburt, "UHD185." [Online]. Available:http://cubert-gmbh.de/wp-content/uploads/UHD-185.pdf. [Accessed: 21-Feb-2016].

[8] BaySpec, "OCI™-2000 Snapshot Handheld Hyperspectral Imager - BaySpec." [Online]. Available:http://www.bayspec.com/spectroscopy/snapshot-hyperspectral-imager/. [Accessed: 21-Feb-2016].

[9] Horiba, "Verde™ Hyperspectral Imaging Camera - Horiba Explore the future." [Online]. Available:http://horiba.escapedoo.webfactional.com/Products/Verde-Hyperspectral-Imaging-Camera. [Accessed: 21-Feb-2016].

[10] IMEC, "IMEC Hyperspectral Snapshot Imager." [Online]. Available:http://www2.imec.be/content/user/File/NEW/Research/Image sensors and vision systems/Hyperspectral imaging/UPDATE 2 imec snapshot imager.pdf. [Accessed: 21-Feb-2016].

[11] G. R. Arce, D. J. Brady, L. Carin, H. Arguello, and D. S. Kittle, "Compressive coded aperture spectral imaging: An introduction," *IEEE Signal Process. Mag.*, vol. 31, no. 1, pp. 105–115, 2014.

[12] A. A. Wagadarikar, R. John, R. M. Willett, and D. J. Brady, "Single disperser design for coded aperture snapshot spectral imaging," *Appl. Opt.*, vol. 47, pp. B44-B51, 2008.

[13] M. E. Gehm, R. John, D. J. Brady, R. M. Willett, and T. J. Schulz, "Single-shot compressive spectral imaging with a dual-disperser architecture.," *Opt. Express*, vol. 15, no. 21, pp. 14013–14027, 2007.

[14] X. Lin, G. Wetzstein, Y. Liu, and Q. Dai, "Dual-Coded Compressive Hyper-Spectral Imaging," no. 1, pp. 5–7, 2014.

[15] L. Wang, Z. Xiong, D. Gao, G. Shi, and F. Wu, "Dual-camera design for coded aperture snapshot spectral imaging.," *Appl. Opt.*, vol. 54, no. 4, pp. 848–58, 2015.

[16] Y. Wu, I. O. Mirza, G. R. Arce, and D. W. Prather, "Development of a digital-micromirror-device-based multishot snapshot spectral imaging system.," *Opt. Lett.*, vol. 36, no. 14, pp. 2692–2694, 2011.

[17] D. S. Kittle, "Design and fabrication of an ultraviolet-visible coded aperture snapshot spectral imager," *Opt. Eng.*, vol. 51, no. 7, p. 71403, 2012.

[18] A. A. Wagadarikar, N. P. Pitsianis, X. Sun, and D. J. Brady, "Spectral image estimation for coded aperture snapshot spectral imagers," vol. 7076, p. 707602, 2008.

[19] A. A. Wagadarikar, N. P. Pitsianis, X. Sun, and D. J. Brady, "Video rate spectral imaging using a coded aperture snapshot spectral imager.," *Opt. Express*, vol. 17, no. 8, pp. 6368–6388, 2009.

[20] D. S. Kittle, K. Choi, A. A. Wagadarikar, and D. J. Brady, "Multiframe image estimation for coded aperture snapshot spectral imagers.," *Appl. Opt.*, vol. 49, no. 36, pp. 6824–6833, 2010.

[21] A. A. Wagadarikar, "Compressive Spectral and Coherence Imaging," *Ph.D dissertation*, Department of Electrical and Computer Engineering, Duke University, 2010.